# TIMP1 Contributes to Ovarian Anomalies in Both an MMP-Dependent and -Independent Manner in a Rat Model[1]

## Julie A.W. Stilley[3,4] and Kathy L. Sharpe-Timms[2,3,4]

[3]The Department of Obstetrics, Gynecology and Women's Health, School of Medicine, the University of Missouri, Columbia, Missouri

[4]Division of Animal Sciences, College of Agriculture, Food and Natural Resources, the University of Missouri, Columbia, Missouri

## ABSTRACT

Ovulatory dysfunction occurs in women with endometriosis, yet the mechanisms are unknown. We have shown that endometriotic lesions synthesize and secrete tissue inhibitor of metalloproteinase (TIMP) 1 into the peritoneal cavity in humans and a rat model of endometriosis, where excess TIMP1 localizes in the ovarian theca in endometriosis and modulating peritoneal TIMP1 alters ovarian dynamics. Here, we evaluated whether mechanisms whereby excessive peritoneal fluid TIMP1 negatively impacts ovarian function are matrix metalloproteinase (MMP)-dependent and/or MMP-independent actions. Rats were treated with a mutated TIMP1 without MMP inhibitory function (Ala-TIMP1), wild-type TIMP1 (rTIMP1), or PBS. Rats treated with Ala-TIMP1 or rTIMP1 had fewer antral follicles, fewer new corpora lutea, and the presence of luteinized unruptured follicle syndrome compared with PBS rats. Ala-TIMP1 and rTIMP1 differentially caused downstream changes in gene expression and protein localization related to ovulation, as measured by whole-genome microarray with quantitative real-time PCR validation and immunohistochemistry. More vascular endothelial growth factor and FN were expressed and localized in ovaries of Ala-TIMP1-treated rats compared to rTIMP1- and PBS-treated rats inferring MMP-independent functions. Less caspase 3 localized in ovaries of rTIMP1 compared with the other two groups, and was thus dependent on MMP action. Furthermore, after coimmunoprecipitation, more CD63 was bound to TIMP1 in ovaries of rats treated with Ala-TIMP1 than in rTIMP1-treated rats, providing evidence for another MMP-independent mechanism of ovulatory dysfunction. We predict that MMP-dependent and MMP-independent events are involved in improper fortification of the follicular wall through multiple mechanisms, such as apoptosis inhibition, extracellular matrix components and angiogenesis. Collectively, excessive peritoneal TIMP1 causes changes in ovarian dynamics, both dependently and independently of MMP inhibition.

*endometriosis, extracellular matrix, ovary, ovulation*

## INTRODUCTION

Endometriosis-associated subfertility is connected with many reproductive anomalies including ovulatory dysfunction leading to fewer oocytes being ovulated and the presence of luteinized unruptured follicle (LUF) syndrome (LUFS), but the mechanisms causing these reproductive anomalies are unknown [1–3]. Due to limitations associated with preclinical, randomized, controlled studies affecting the function of human ovaries, animal models have been utilized to study the mechanisms underlying the pathophysiologies of endometriosis [1, 2]. Pathophysiologies of human endometriosis, including pain and subfertility, are replicated in a rat model of endometriosis with surgically induced disease (Endo) [2–6]. Research from our laboratory has found ovulatory dysfunction, including reduced numbers of antral follicles, fewer oocytes ovulated, and the presence of LUFs in Endo compared with control rats with a control surgery (Sham) [5, 6].

Matrix metalloproteinases (MMPs) and their inhibitors (tissue inhibitors of metalloproteinases [TIMPs]) have been studied in the pathophysiologies of endometriosis occurring in both women [7–10] and in a rat model [5, 6, 9]. Both eutopic and ectopic endometrium synthesize and secrete MMPs and TIMPs [9, 10]. Importantly, TIMP1 represents 10%–15% of total proteins secreted into the peritoneal cavity by human endometriotic lesions and rat endometriotic implants [9, 10]. TIMP1 synthesized and secreted from the lesions is likely acting directly on extracellular matrix (ECM) remodeling of the lesions themselves [9]. Furthermore, this excess TIMP1 could cause disruption of normal MMP/TIMP functions throughout the reproductive tract.

Precise choreography of expression and action of MMPs and TIMPs throughout the reproductive cycle is required for normal ovarian function [11–15]. TIMPs have a two-domain structure with N- and C-terminal regions, each with unique functions [16]. The N-terminal domain is sufficient for inhibition of MMPs. However, unique MMP-independent features of TIMPs in regulation of apoptosis, cell growth, and angiogenesis are facilitated in part by specific protein-protein interactions mediated by their C-terminal domain [16–18]. For example, Chirco et al. identified CD63, a cell surface-binding member of the tetraspannin family, as a TIMP1-binding protein [16]. Experimental downregulation of CD63 effectively reduced TIMP1 binding to the cell surface of human breast epithelial MCF10A cells, and consequently reversed TIMP1-mediated activation of cell survival signaling and its inhibition of apoptosis, demonstrating the functional significance of TIMP1 interaction with CD63.

Previous studies from our laboratory have shown that more endometriotic TIMP1 from the peritoneal fluid localized to the theca layer in antral follicles of Endo rats compared with Sham rats [5, 6], and is associated with reduced numbers of follicles,

ovulatory dysfunction, and poor embryo quality. Introduction of a TIMP1 function-blocking antibody into the peritoneal fluid mitigated the impact of endometriosis on the ovary. Reducing TIMP1 function in Endo rats restored the number of follicles, corpora lutea (CLs), and zygotes to levels observed in Sham rats. Conversely, increasing TIMP1 by intraperitoneal injection was able to block ovarian function as described. Sham rats treated with TIMP1 had numbers of follicles, CLs, and zygotes reduced to levels similar to those of Endo rats. An increase of TIMP1 protein localization, but not gene expression, was seen in rats treated with TIMP1, suggesting that TIMP1 from the peritoneal milieu was able to enter into antral follicles. While this work provided a foundation for the role of endometriotic TIMP1 in ovulatory dysfunction, it is not clear if TIMP1 is working through MMP-dependent or -independent mechanisms. Therefore, the objective of this study was to evaluate TIMP1 in ovulatory dysfunction in regard to its MMP-dependent and -independent actions in the occurrence of LUFS, the reduction in numbers of antral follicles or CLs.

## MATERIALS AND METHODS

### Animal Management

Mature female Sprague-Dawley rats (250 g; Harlan, Indianapolis, IN) exhibiting regular 4- to 5-day estrous cycles were housed in an environmentally controlled room with a 14L:10D cycle. All rats were allowed an acclimation period in the vivarium for 14 days. The experiments were conducted with the approval of the University of Missouri Institutional Animal Care and Use Committee and in accordance with the National Research Council's *Guide for Care and Use of Laboratory Animals* [19].

### In Vivo Treatments and Validation of Reproductive Cyclicity

Rats received intraperitoneal injections (200 μl/injection) of mutated TIMP1, where the N-terminal mutation included an addition of an alanine residue (Ala-TIMP1; 2.8 μg/kg; a kind gift of Dr. William G. Stetler-Stevenson, National Institutes of Health, Bethesda, MD) to prevent MMP inhibition, also tagged with poly-histidine [20, 21] (n = 8), recombinant rat TIMP1 (rTIMP; 2.8 μg/kg; R & D Systems, Minneapolis, MN; n = 7), or PBS (n = 7) as a control. The doses of the TIMP1 treatments were based on in vivo levels of endogenous TIMP1 in peritoneal fluid of Endo rats, as in our previous experiments [6]. Treatments (intraperitoneal injections) started on the morning of the second proestrus after LHRH synchronization, as previously described [6] (Sigma-Aldrich Co., St. Louis, MO), and were repeated every 3 days for a total of three injections.

Vaginal cytology was monitored daily in all rats as an indication of reproductive cyclicity [22]. Postovulatory Endo and Sham rats were euthanized in a $CO_2$ chamber between 0700 and 0800 h, with general necropsy observations noting no gross differences among treatments. Only the right ovary (nearest to the treatment injection site) was used for experimentation, based on the endometriosis model in rats in which only the right ovary is present [2]. One-half of the ovary was fixed for histology in 10% buffered formalin before paraffin embedding. The remaining half was snap frozen in liquid nitrogen for nucleic acid and proteomic analysis.

### Experimental Supplies

All commercially available products were used as per manufacturers' recommendations unless otherwise noted. This includes products for both nucleic acid and proteomic experiments.

### Quantification of Follicle and CL Numbers

Differences in the numbers of follicles and CLs between treatment groups (Ala-TIMP1 [n = 8]; rTIMP1 [n = 7]; PBS [n = 7]) were evaluated histologically and quantified morphometrically, as described previously, spanning 408 μm of the ovary [6]. These morphometric calculations were based on size, so that no antral follicle, CL, or LUF was counted more than once in each ovary. New CLs were identified by size, presence of blood, presence of basement membrane, and the lack of many infiltrating fibroblast cells. All morphological and morphometric analyses were performed by the two investigators blinded to the study group. Differences in the numbers of follicles and in the number of new CLs between treatments were analyzed by one-way ANOVA and Student-Newman-Keul test for post hoc pairwise multiple comparisons.

### Downstream Gene Expression after TIMP1 Treatment with and Without MMP Activity

Total RNA was isolated from one-quarter of the ovary (~20 mg) using the RNeasy Mini Kit (Qiagen, Valencia, CA). A TotalPrep Kit was used to synthesize biotin-labeled cRNA (Illumina, Inc., San Diego, CA). Biotin-labeled cRNA (750 ng) from individual rats was hybridized to the Illumina RatRef-12 whole-genome microarray chip by the MU DNA Core, and analyzed using the Illumina BeadArray Reader.

For statistical analysis, the log fold change of ovarian mRNA levels was computed, along with adjusted $P$ values and the estimated log-odds ratios of differential expression, as previously described [23]. Due to small sample sizes, samples with a fold change greater than 1 and a $P$ value $\leq 0.05$ were considered differentially expressed. Genes of interest were selected using the DAVID Bioinformatics Resources 6.7 pathway analysis [24, 25] and biological relevance to known pathways in ovulation, as evidenced in the literature.

Genes from the whole-genome microarray chip chosen for further gene expression analysis included: anti-mullerian hormone (*Amh*, assay id Rn00563731_g1), caspase 3 (*Casp3*, Rn00563902_m1), collagen, type III, α 1, (*Col3a1*, Rn01437681_m1), collagen, type XVIII, alpha 1 (*Col18a1*, Rn01428995_m1), fibronectin 1 (*Fn1*, Rn00569575_m1), PYD and CARD domain-containing protein (*Pycard*, Rn00597229_g1), Mothers against deca-pentaplegic homolog 1 (*Smad1*, Rn00565555_m1), synaptic vesicle glycoprotein 2B (*Sv2b*, Rn01478297_m1), transforming growth factor beta 1 (*Tgfb1*, Rn00572010_m1), and vascular endothelial growth factor (*Vegfa*, Rn01511601_m1).

The mRNA levels of these genes were confirmed by quantitative real-time PCR (Q-PCR), as previously described [6]. Ovarian RNA (500 ng) from a different quarter of the same ovary from each rat (Ala-TIMP1 [n = 8]; rTIMP1 [n = 7]; PBS [n = 7]) was reverse transcribed into cDNA using the High-Capacity cDNA Reverse Transcription Kit (Applied Biosystems, Carlsbad, CA). Note that this is an alternative method for isolating RNA than that performed for isolating the RNA for the microarray experiments (RNeasy Mini Kit; Qiagen), further validating the fidelity of these data. Q-PCR was performed using Taqman PCR Mix from Applied Biosystems in an ABI 7500 Real-Time PCR System. Ribosomal 18s gene expression was used to normalize the target gene expression data. Validated primer/probe sets were purchased from Applied Biosystems. All samples were tested in triplicate on the same 96-well plate for each individual gene. Statistical differences were calculated using the ΔCt method (Ct of target gene − Ct of 18s housekeeping gene expression). Hence, the lower the ΔCt, the greater the amount of gene transcript present in a sample. Fold changes in gene expression are reported. An ANOVA was performed with post hoc pairwise comparisons performed using the Student-Newman-Keuls test. Genes with a $P$ value trend demonstrating a trend toward significance ($P = 0.05$–0.10) in the microarray analyses (caspase 3, collagen III a1) were individually analyzed by Student $t$-test.

### Proteins Complexed with TIMP1 with and Without MMP Inhibitory Activity

Using the NE-PER Nuclear and Cytoplasmic Extraction Kit (Thermo Fisher Scientific, Waltham, MA), snap-frozen ovarian tissues (20 mg) were homogenized, and cytoplasmic and nuclear protein fractions were extracted. Total protein was evaluated by the DC Protein Assay (Bio-Rad Laboratories, Hercules, CA).

Cytoplasmic fractions were subjected to coimmunoprecipitation. An anti-TIMP1 rabbit polyclonal antibody, designed to recognize TIMP1 amino acids 58–207 (Santa Cruz Biotechnologies, Inc., Santa Cruz, CA), was purified using Pierce Antibody Clean-up Kit (Thermo Fisher Scientific). A total of 50 μg purified antibody was used per 750 μg of total protein to immunoprecipitate TIMP1. The Pierce Co-Immunoprecipitation Kit was used to carry out immunoprecipitation procedures (Thermo Fisher Scientific). Using kit components, a negative control was created where anti-TIMP1 bound to the resin was quenched, eliminating specific binding sites of the antibody. All proteins precipitated by the quenched antibody control were considered nonspecific binding.

Western blot analysis for CD63 was performed as previously described [6]. Total protein (2 mg) was separated by 12% SDS-PAGE and electrophoretically transferred to a nitrocellulose membrane. The membrane was incubated with polyclonal rabbit anti-rat CD63 (1:100 ng/ml; Santa Cruz Biotechnologies) at 4°C overnight. A biotinylated secondary antibody, anti-rabbit IgG (5 mg/ml; Vector Laboratories, Burlingame, CA), was used before visualization of the bands by an ABC kit (Vector Laboratories) with diaminobenzidine.
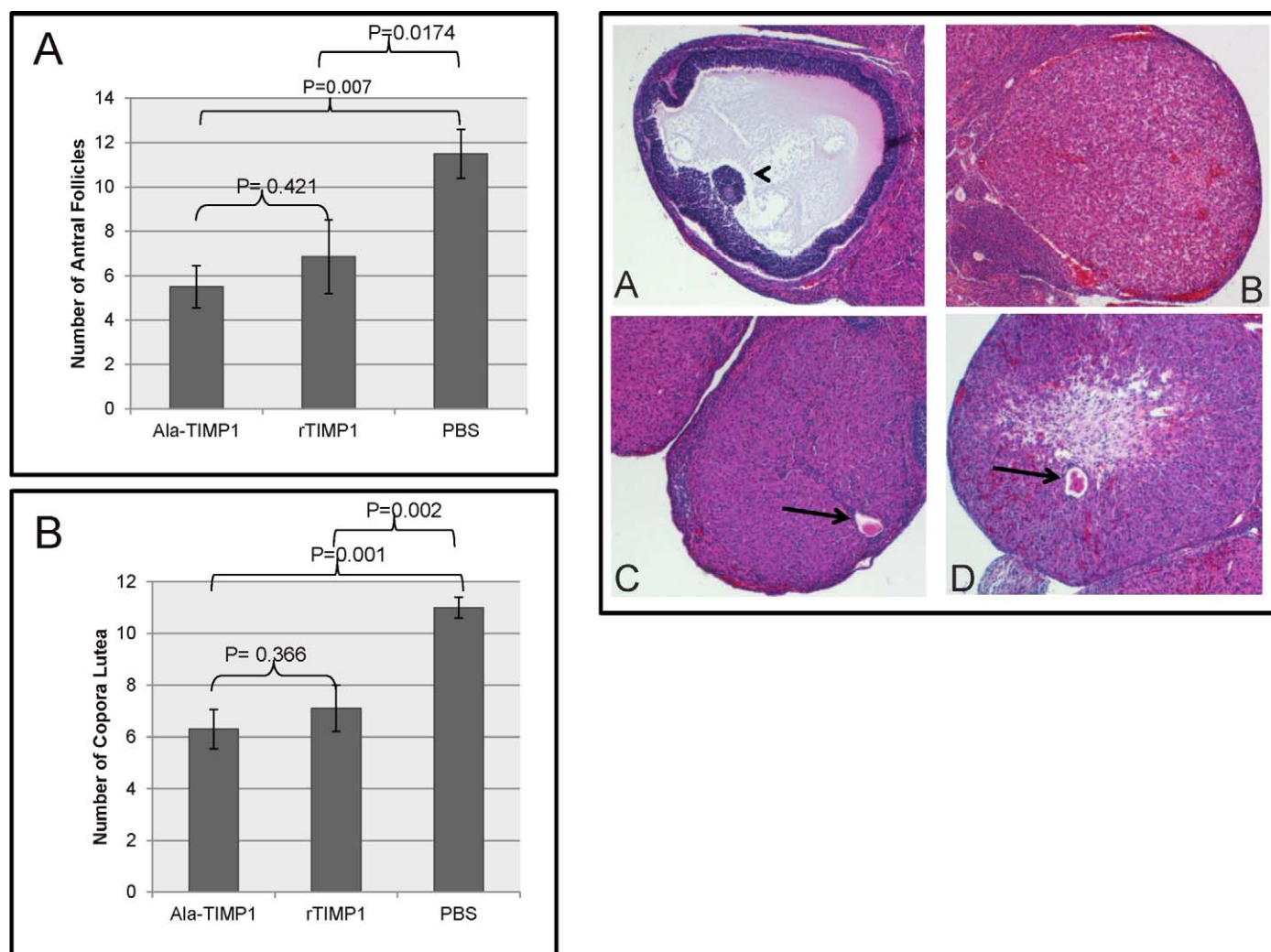
FIG. 1. Treatment with TIMP1 influences ovarian dynamics. Bar graphs: **A**) treatment with TIMP1, regardless of MMP-inhibitory status (Ala-TIMP1 or rTIMP1), resulted in fewer antral follicles compared to vehicle (PBS) treatment; **B**) both TIMP1 treatments also reduced the number of new CLs. Photomicrographs: **A**) normal antral follicle from PBS-treated rat, which may ovulate in the next cycle (arrowhead: oocyte); **B**) normal CL from a PBS-treated rat (this CL has newly formed); **C**) appearance of LUFs in rTIMP1-treated rat CL (arrow: oocyte entrapped in CL); **D**) appearance of LUFs in Ala-TIMP1-treated rat newly forming CL (arrow: retained oocyte in CL). Original magnification ×100.

Western blot analysis for the histidine tag located on the mutated Ala-TIMP1 was performed using the left ovary. This confirmed the presence of the mutated protein in rats treated with Ala-TIMP1, but not rTIMP1 or PBS (data not shown).

### Immunolocalization of Proteins Corresponding to Gene Products Identified by Microarray and Q-PCR

Immunohistochemistry (IHC) was performed as previously described [5]. Formalin-fixed, paraffin-embedded, and routinely processed tissues sectioned at 8 μM were incubated with antibodies, including rabbit polyclonal anti-TIMP1 (1 μg/ml; Cell Applications, Inc., San Diego, CA), rabbit polyclonal anti-6× histidine (100 μg/ml; Abcam, Cambridge, MA), mouse monoclonal anti-VEGF (2 μg/ml; Santa Cruz Biotechnologies), or mouse monoclonal anti-FN1 (2 μg/ml; Santa Cruz Biotechnologies), and mouse monoclonal anti-CASP3 (2 μg/ml; Santa Cruz Biotechnologies) at 4°C overnight. Appropriate anti-rabbit or anti-mouse biotinylated secondary antibodies were used (Vector Laboratories), and then fluorescein isothiocyanate-labeled avidin was used to visualize protein localization (Vector Laboratories). Tissues were then incubated with 4′,6-diamidino-2-phenylindole to stain cell nuclei.

Immunofluorescence of protein relating to the genes identified by Q-PCR was quantified using Image J software [26]. Each tissue represented on the image was traced and measured for comparison. All data were reported as mean intensity per area and compared using ANOVA and Student-Newman-Keuls for post hoc testing.

## RESULTS

### Exogenous TIMP Altered Ovarian Function Regardless of MMP-Inhibitory Activity

Numbers of antral follicles quantified was similar between Ala-TIMP1 and rTIMP1 ($P = 0.421$), but significantly lower than PBS treatment ($P = 0.007$ and 0.017, respectively; Fig. 1). Likewise, the numbers of newly formed CLs were similar between Ala-TIMP1- and rTIMP1-treated rats ($P = 0.631$), but lower than in PBS-treated rats ($P = 0.001$ and 0.004, respectively). LUFs were found in ovaries of Ala-TIMP1-treated rats (38%) and rTIMP1-treated rats (29%), but not in ovaries of those treated with PBS (0%).

### Downstream mRNA Levels Were Different in MMP-Independent TIMP1-Treated Ovaries Compared with Treatment with Fully Functional TIMP1

Of the 22 000 genes analyzed on the microarray, 50 genes were differentially expressed when comparing all treatments (Supplemental Fig. S1; available online at www.biolreprod.

TABLE 1.   Quantification of relative mRNA expression levels of selected genes by quantitative real-time RT-PCR.[a]

| Gene symbol | ANOVA $P$ value | Fold change (if applicable) | $P$ value of fold change[b] | Kegg pathway cluster |
|---|---|---|---|---|
| *Amh* | 0.773 | | | TGFB |
| ***Casp3**\** | **0.088** | Ala-TIMP1 v. rTIMP1 - **2.1** | **0.05** (*t*-test) | Apoptosis |
| ***Col3a1*** | **0.054** | Ala-TIMp1 v. rTIMP1 - **2.3** | **0.069** (*t*-test) | ECM, TGFB, Integrin |
| *Col18a1* | 0.287 | | | ECM, Apoptosis, Angiogenesis, Integrin |
| ***Fn1**\** | **0.048** | Ala-TIMP1 v. rTIMP1 - **3.9** | **0.04** | ECM, Apoptosis, Integrin |
| | | AAla-TIMP1 v. PBS - 1.6 | 0.424 | |
| | | rTIMP1 v. PBS - 2.5 | 0.112 | |
| | | | (SNK) | |
| *Pycard* | 0.749 | | | Apoptosis |
| *Smad1* | 0.324 | | | TGFB |
| *Sv2b* | 0.111 | | | ECM |
| *Tgfb1* | 0.445 | | | TGFB, Apoptosis |
| ***Vegfa**\** | **0.010** | Ala-TIMP1 v. rTIMP1 - **1.9** | **0.041** | Angiogenesis, Apoptosis |
| | | Ala-TIMP1 v. PBS - **2.9** | **0.008** | |
| | | rTIMP1 v. PBS - 1.5 | 0.208 | |
| | | | (SNK) | |

[a] Bold indicates trend or significance; *indicates selection for protein valuation.
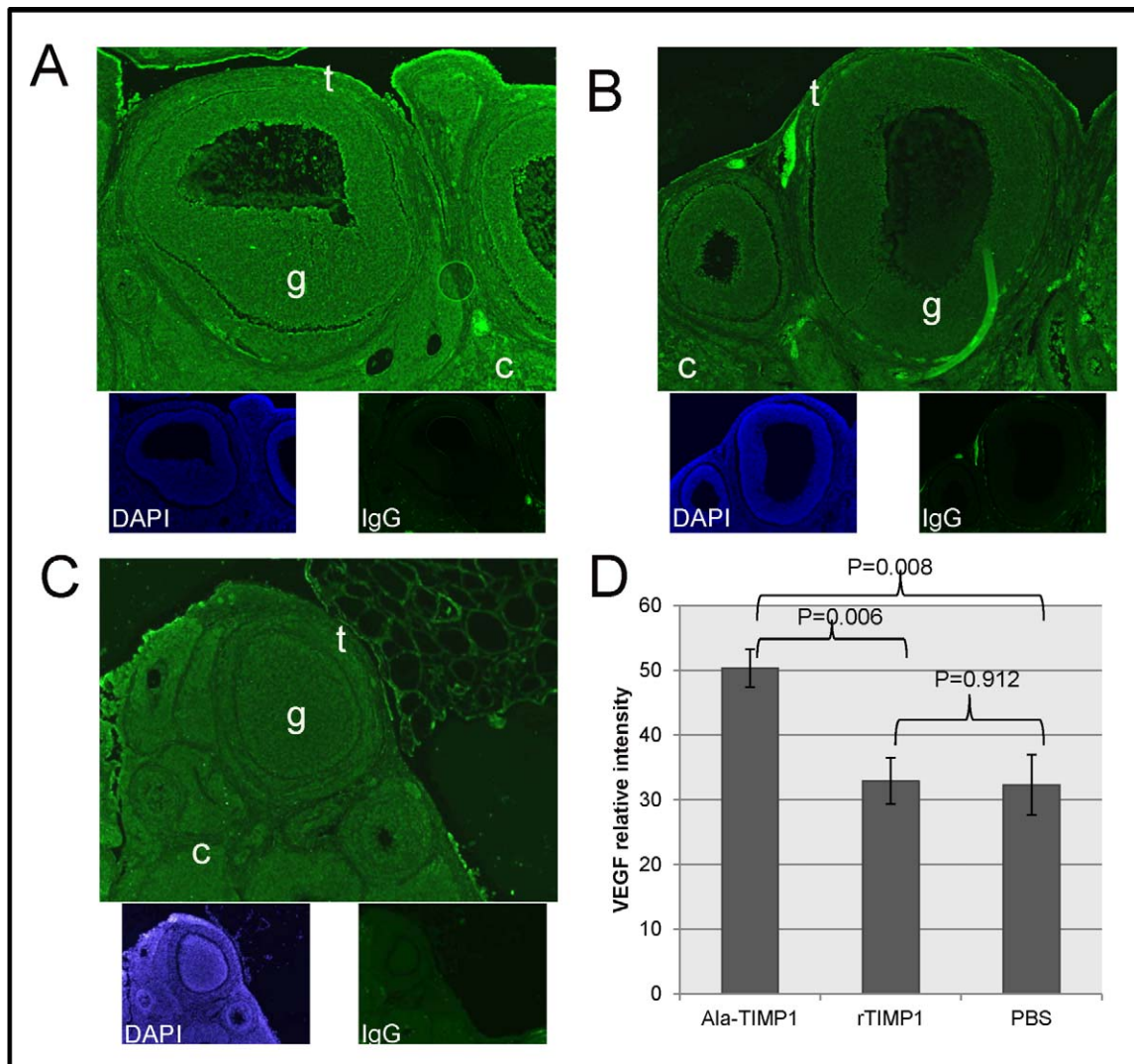[b] *t*-test, Student *t*-test; SNK, Student Newman-Keul test.



FIG. 2.   VEGF protein immunolocalization and quantification by morphometric analysis. **A**) More fluorescent intensity of VEGF (green) localized in ovaries from Ala-TIMP1-treated rats compared with ovaries from (**B**) rTIMP1-treated rats or (**C**) PBS-treated rats. Theca (t), granulosa (g), and ovarian cortex (c) are marked. The bottom images in **A**, **B**, and **C** show nuclear staining (4′,6-diamidino-2-phenylindole [DAPI], blue) and a negative control using IgG, as indicated. Original magnification ×100. **D**) Quantitative analysis shown in graph (ANOVA: $P = 0.004$).

Article 47
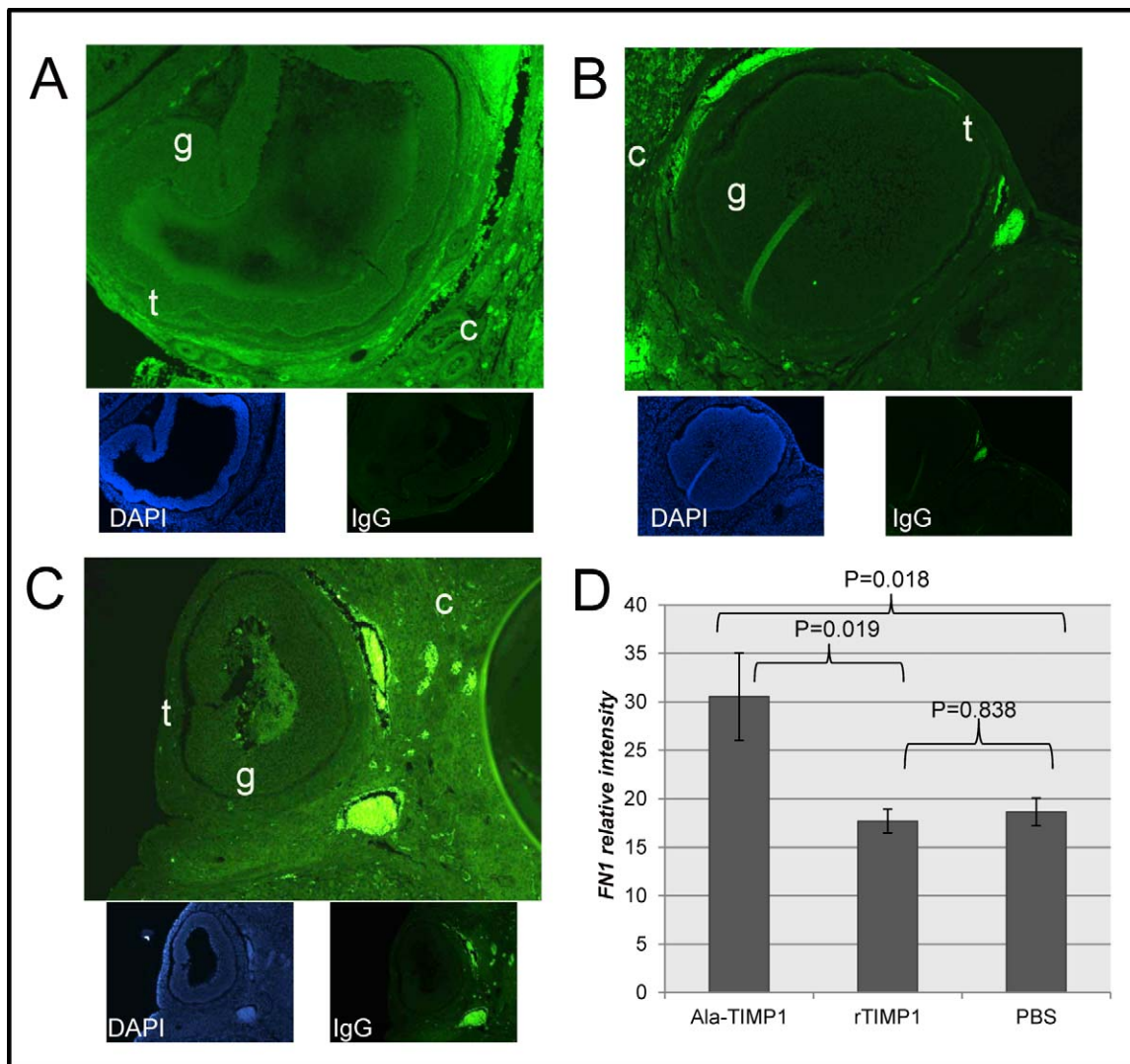
FIG. 3. FN1 protein immunolocalization (100×) and quantification by morphometric analysis. Fluorescence intensity of FN1 (green) was significantly greater in ovaries from (**A**) Ala-TIMP1-treated rats compared with (**B**) rTIMP1-treated rats or (**C**) PBS-treated rats. Theca (t), granulosa (g), and ovarian cortex (c) are marked. The bottom images in each panel show DAPI localization (blue) and a negative control using IgG, as indicated. Original magnification ×100. **D**) Quantitative analysis shown in graph (ANOVA: $P = 0.014$).

org). The 50 genes were then functionally clustered by KEGG analysis, revealing several pathways in ovulation that may be affected, including TGF-beta signaling implicated in ovulatory failure [27], ECM-receptor interaction, integrin signaling pathway, regulation of apoptosis, and angiogenesis. From these genes and clusters, 10 genes were selected for further analysis using Q-PCR (Table 1). Overall, the fold change in gene levels detected by Q-PCR was of the same magnitude and direction as found by microarray.

*Protein Localization of Targets Identified by mRNA Expression Were Different in MMP-Independent TIMP1-Treated Ovaries Compared with Treatment with Fully Functional TIMP1*

Based on differential gene expression and functional relevance to ovulation, three targets were chosen to be further evaluated by analyzing protein in the ovary. Protein localization of those targets (VEGF, FN1, and CASP3) was performed

by IHC. These targets were selected for their roles in angiogenesis, ECM, and apoptosis, respectively.

VEGF localized in the ovary, including the follicular theca and granulosa cells, plus the new CL and cells of the cortex. Overall, more VEGF localized in the ovaries of Ala-TIMP1-treated rats than in those of rTIMP1-treated ($P = 0.006$) or PBS-treated rats ($P = 0.008$; Fig. 2). However, VEGF localization did not differ between rTIMP1-treated and PBS-treated rats ($P = 0.912$).

Fibronectin 1 fluorescence intensity was also greater in the ovaries of Ala-TIMP1-treated rats compared with rTIMP1-treated ($P = 0.018$; Fig. 3) and PBS-treated rats ($P = 0.019$), but did not differ between rTIMP1-treated and PBS-treated rats ($P = 0.838$). The staining pattern preferentially localized to theca cells, but was also present in lesser amounts in the granulosa cells, CL and cortex of the ovary.

Caspase 3 protein fluorescence intensity was also increased in all cell types of the ovaries of Ala-TIMP1 rats compared with rTIMP1 rats ($P = 0.019$; Fig. 4). However, there was not an increase between Ala-TIMP1-treated rats and PBS-treated
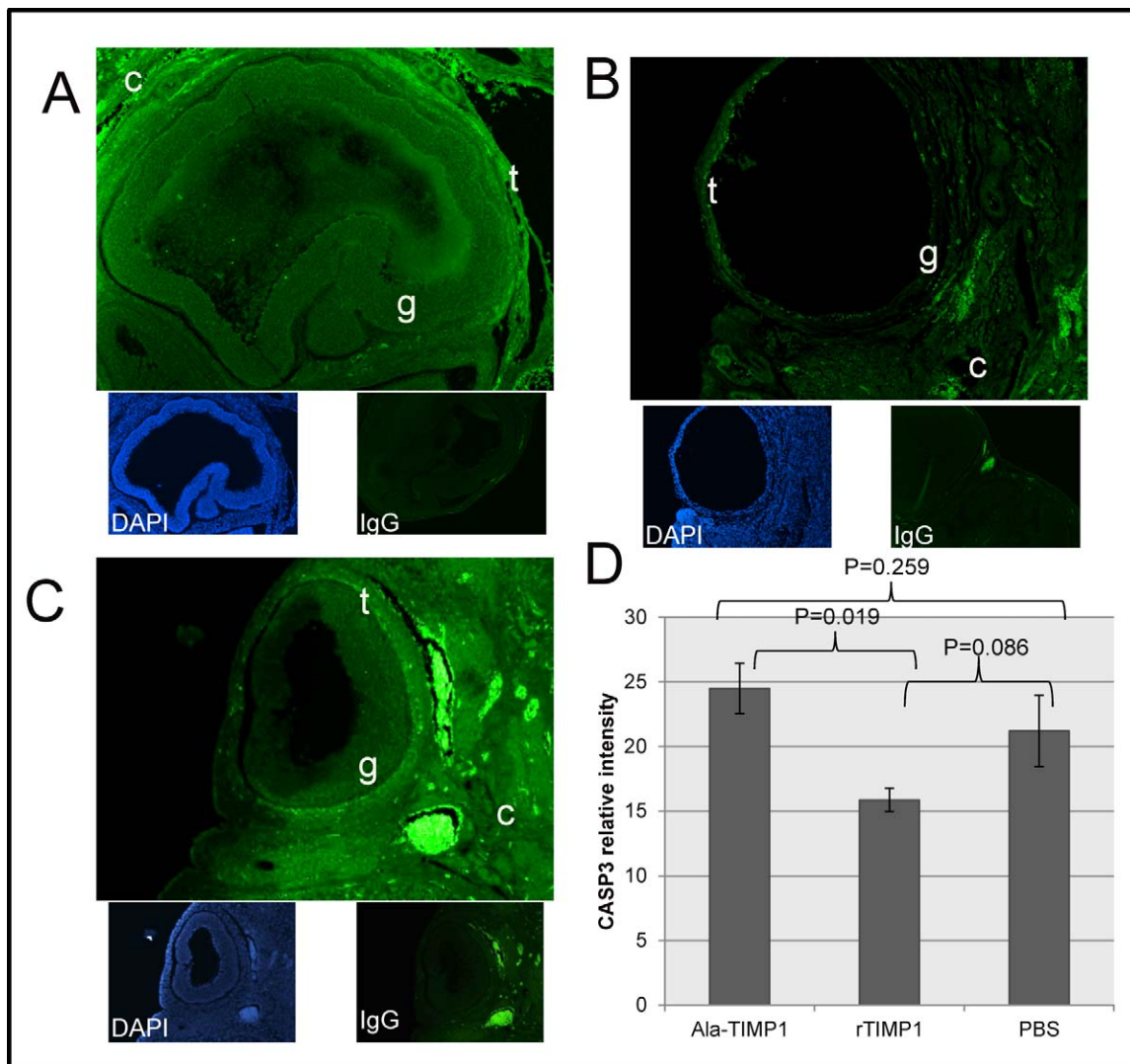
5

FIG. 4. CASP3 protein immunolocalization (100×) and quantification by morphometric analysis. Fluorescence intensity of CASP3 was greater in (**A**) Ala-TIMP1-treated rats compared with (**B**) rTIMP1-treated rats. However, there was not a difference between PBS-treated rats and Ala-TIMP1-treated rats or rTIMP1-treated rats (**C**). Theca (t), granulosa (g), and ovarian cortex (c) are marked. The bottom images in each panel show nuclear staining (DAPI, blue) and a negative control using IgG, as marked. Original magnification ×100. **D**) Quantitative analysis shown in graph (ANOVA: $P = 0.024$).

rats ($P = 0.259$). There was a trend for caspase 3 fluorescence intensity to be greater in the ovaries of rTIMP1-treated rats than PBS-treated rats ($P = 0.089$). These increases in protein localization help substantiate the increase in mRNA level found in these studies. Levels of mRNA were correlated with protein fluorescence intensity using Pearson correlation, where a low ΔCt correlated with a high protein fluorescence intensity ($-0.28$, $P = 0.045$). Recall that a lower ΔCt indicates more mRNA; thus, as gene expression increased, protein localization intensity did as well.

*Proteins Coimmunoprecipitated with TIMP1 Depends on MMP-Inhibitory Status*

Cytoplasmic fractions of ovarian lysate proteins complexed to TIMP1 were immunoprecipitated. Proteins from eluates from the coimmunoprecipitation were subjected to Western blot analysis to visualize the presence of CD63 complexed to TIMP1. More CD63 was complexed to TIMP1 in the ovarian eluates of Ala-TIMP1-treated rats than in that of rTIMP1-

treated rats, showing that CD63 does, in fact, bind to the TIMP1 independently of MMPs (Fig. 5).

## DISCUSSION

The results of these studies provide evidence that inappropriate localization of TIMP1 in the ovary contributes to ovulatory failure in both MMP-dependent and -independent mechanisms. Exogenous TIMP1, with or without MMP-inhibitory activity, negatively impacted ovarian dynamics through disruption of folliculogenesis, as shown by the reduced numbers of antral follicles in rats treated with Ala-TIMP1 or rTIMP1 compared with controls. Numbers of new CLs were also reduced, indicating that treatments may also have affected the numbers of follicles ovulated soon after treatment began. The rapid effect of exogenous TIMP1 on ovulatory function illustrates the sensitivity of the ovary to disruption of the ECM remodeling during ovulation. Considering these data, the ability of TIMP1 to contribute to ovulatory disruption in endometriosis may be more complex than previously anticipated. It is not clear exactly how this exogenous TIMP1 is able
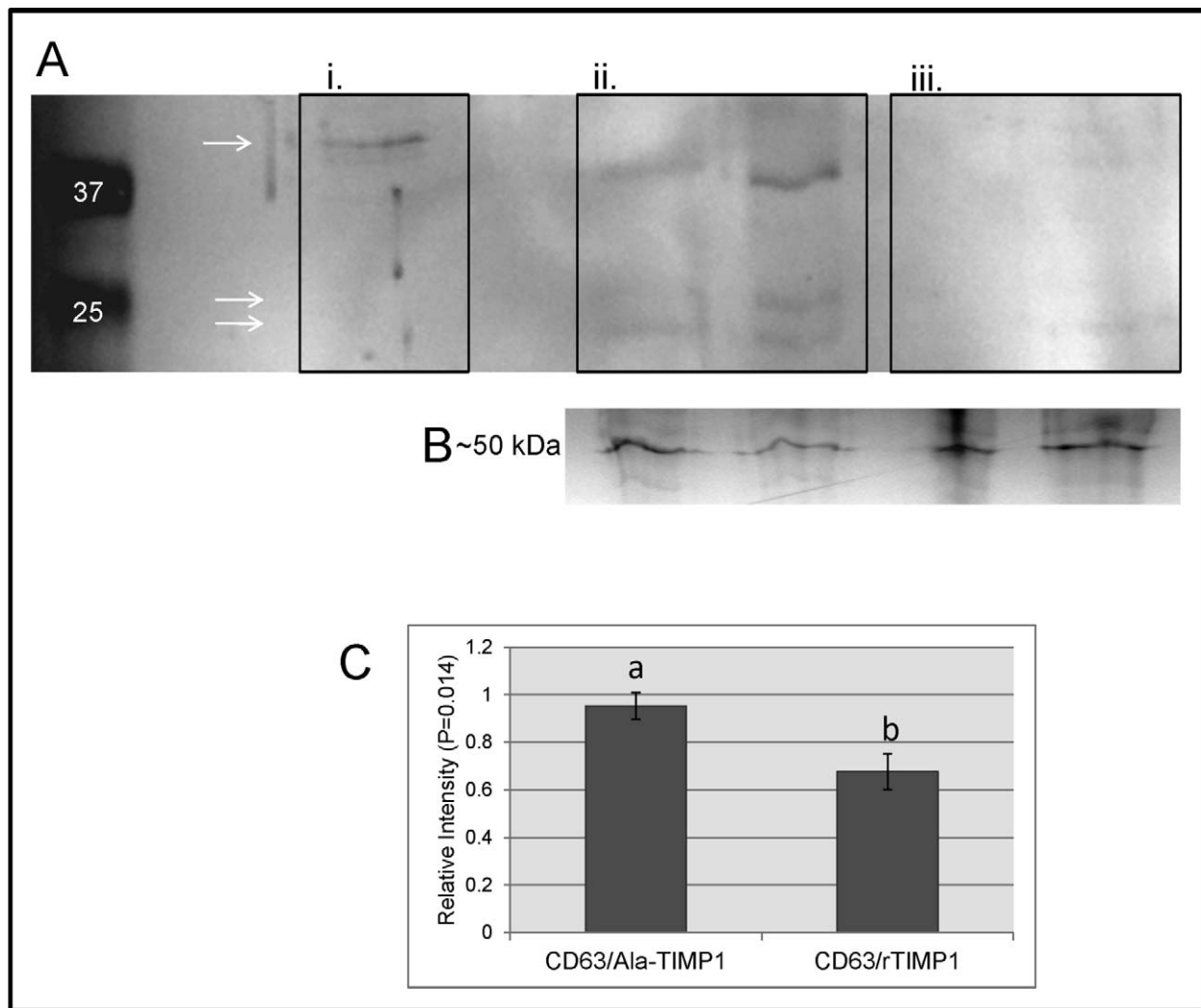
FIG. 5. CD63 Western blot analysis of coimmunoprecipitated proteins. **A**) Representative Western blot with visible bands of CD63. Lane 1 is a molecular marker. Lane marked i. is neat ovarian protein extracts as a positive control. Lanes marked ii. are Ala-TIMP1 eluates from TIMP1 coimmunoprecipitation. Lanes marked iii. are rTIMP1 eluates from TIMP1 coimmunoprecipitation. Bands are expected at 24–25 and 42 kDa, as indicated by the arrows (AbCam). **B**) Coomassie blue-stained gel of albumin of about 50 kDa before immunoprecipitation as a load control. **C**) Ala-TIMP1 rats had more relative intensity of CD63 in coimmunoprecipitation eluates using Western blot analysis than rTIMP1 rats ($P = 0.014$).

to access the ovarian follicles—perhaps by transport by the circulatory system or by direct transport into the cell.

The presence of LUFs in the treated animals provides further evidence for the involvement of TIMP1 in the potential risks of ovulatory failure in women with endometriosis [28–30]. Even after short-term exposure to exogenous TIMP1 at endometriotic levels of endogenous TIMP1, these rats showed anomalies in ovarian function, which is in agreement with findings from our previous study [6]. In this case, the presence of LUFs in rats treated with MMP-independent Ala-TIMP1 indicates that ECM components are being misregulated beyond remodeling by MMPs alone.

While the histology of the two exogenous TIMP1 treatment groups appeared similar, it is likely that these groups were acting through different molecular mechanisms. The genome-wide microarray is a useful tool in discovering the downstream effects of MMP-independent functions of exogenous TIMP1 in the ovary. After confirmation by Q-PCR, genes influenced by MMP-independent functions of TIMP1 included genes involved in ECM receptor signaling, apoptosis, and angiogenesis.

Ala-TIMP1 upregulated the expression and localization of VEGF compared with rTIMP1. VEGF is the hallmark for new vascular growth. During folliculogenesis, the microvascular beds of follicles undergo vast changes to support the growth of the follicle and oocyte [31]. However, shortly before follicular rupture, blood flow stops in the follicular wall where ovulation will occur [31]. TIMP1 appears to directly affect vascularization in the ovary. Mice lacking the *Timp1* gene had greatly reduced vascularity in their ovaries [14]. VEGF is also implicated in the inhibition of apoptosis [32]. Furthermore, VEGF is also regulated by gonadotropins. After withdrawal of LH, Ravindranath et al. noted that VEGF was reduced [33]. These data suggest that, following the LH surge triggering ovulation (at the time that these rats were killed), VEGF should be reduced.

Additionally, VEGF itself has been implicated in subfertility. For example, increased levels of VEGF in follicular fluid of women seeking treatment with assisted reproductive techniques were associated with poor conception rates and fewer oocytes retrieved during assisted reproductive technique procedures [34]. VEGF has also been implicated in endometriosis, specifically as a contributor to peritoneal milieu [35]. Levels

**N-Terminus Actions**

Prevention of
ECM Breakdown
Regulation of
MMPs

Inhibition of
Apoptosis
↓ CASP3
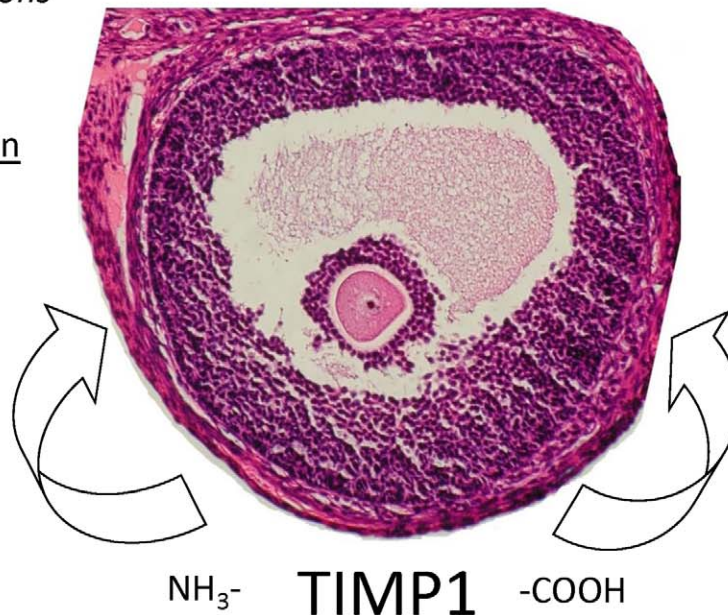
**C-Terminus Actions**

Fortification of
ECM Components
↑FN1
↑ *Col3a1*

Fortification of
Follicular Wall
↑VEGF

Aberrant Timing
of Luteinization
↑CASP3

Inhibition of Apoptosis
of Follicular Wall
↑CD63
↑VEGF

NH₃- **TIMP1** -COOH

FIG. 6. Summary of the roles of TIMP1 in ovulatory dysfunction. TIMP1 contributes to ovulatory failure by MMP-dependent and -independent mechanisms. MMP-dependent functions of TIMP1 regulate MMPs via the N terminus, while independent mechanisms of the C terminus are able to influence downstream gene expression as well as form complexes with other proteins. Specific details of these actions are discussed in the main text. These functions lead to improper fortification of the ECM. Original magnification ×200.

of VEGF in the follicular fluid of women with endometriosis are increased [36]. Our study showed that, in ovarian tissue, elevated concentrations of VEGF are associated with anomalous ovarian function.

Treatment with Ala-TIMP1 also upregulated the gene expression and protein content of FN1 compared with rTIMP1. FN1 is an ECM glycoprotein that binds to integrins and other ECM components [37]. Breakdown of FN1 is important during the extensive tissue remodeling during ovulation [38]. Increased FN1 due to treatment with Ala-TIMP1 may stabilize the ECM instead of allowing for disassembly of the ECM in the follicular wall of an antral follicle. Additionally, while Q-PCR did not detect a significant difference, ovarian levels of the ECM component *Col3a1* [39] mRNA tended ($P = 0.069$) to be higher in ovaries from Ala-TIMP1-treated rats compared with rTIMP1 rats measured by microarray technology and validated by Q-PCR. Although COL3A1 protein localization was not tested, an increased *Col3a1* mRNA in the ovary would also stabilize the ECM, similar to the consequence of increased FN1. These data suggest that TIMP1 can affect ECM components (*Fn1* and *Col3a1*) independently of MMPs. Since Ala-TIMP1 cannot inhibit MMPs, endogenous MMPs should have been able to breakdown these increased ECM components, but they did not. It is possible that the excessive Ala-TIMP1 cannot trigger an overexpression of MMPs; therefore, the excess ECM overwhelms the endogenous enzymes to cause an accumulation.

An increase in CASP3 expression and localization in Ala-TIMP1-treated rats compared with rTIMP1-treated rats is challenging to understand, because TIMP1 has been shown to inhibit apoptosis, yet CASP3 is directly involved in the caspase apoptotic pathway. While not different from PBS-treated rats, it

is possible that exogenous Ala-TIMP1 entering a cell could trigger apoptotic events. However, Dassé et al. reported that TIMP1 causes the differentiation of hematopoietic cells by inducing CASP3 to activate mitogen-activated protein kinase kinase [40]. If Ala-TIMP1, acting through CASP3, is working via this mechanism and causing cell differentiation in the follicle, it is possible that luteinization of the follicular cells could prematurely activate ECM stabilization, preventing follicular rupture and leading to the presence of LUFs.

Conversely, there was a trend in decreasing localization of CASP3 localization in ovaries from rTIMP1-treated rats compared with PBS-treated rats. These data support the work of others suggesting TIMP1 plays a role in inhibiting apoptosis [41]. Furthermore, these data indicate that this potential inhibition in caspase-mediated apoptosis is MMP dependent.

Collectively, these data suggest that endometriotic TIMP1 alters the composition of ECM components and the follicular wall in the preovulatory follicle, thereby preventing successful rupture of the follicle, leading to fewer ovulations and the presence of LUFs. It is likely that downstream events after treatment with TIMP1 work together to aberrantly stabilize ECM components in the follicle, both at the cellular level and at the level of basement membrane, at a time when the follicular wall should be broken down for ovulation [42, 43].

It is known that TIMP1 can bind to CD63, serving as a receptor for intracellular signaling pathways, including gene expression, leading to cell adhesion, motility, and survival [18, 44]. Additionally, TIMP1/CD63 binding on the cell surface can help explain potential exogenous TIMP1 actions, such as those seen previously in our lab. An increase in CD63 binding in the Ala-TIMP1-treated rats provides evidence for another MMP-independent mechanism of ovulatory dysfunction. Focused

Article 47

apoptosis in the precise location of follicular rupture is a normal occurrence immediately before ovulation [45]. Interaction of TIMP1 with CD63 may inhibit apoptosis by working through the FAK pathway [16, 44]. This inhibition may be preventing the normal breakdown of the follicular wall during ovulation. In the case of endometriotic TIMP1, ovulatory failure is likely exacerbated through both MMP-dependent mechanisms (CASP3) and MMP-independent mechanisms (CD63, VEGF) to inhibit normal apoptosis.

There are several limitations in this study, which future work may address. One limitation is the ability to test the MMP-dependent-only interactions of TIMP1. Creation of mutated C-terminus TIMP1 to potentially prevent MMP-independent mechanisms may be possible to test whether ovulatory dysfunction requires MMP-independent functions. Additional limitations include the liberal selections of genes from the microarray; yet, in support of our outcomes, the genes chosen were identified in the literature with roles in ovulation, and were further explored here by Q-PCR and IHC.

Future studies are planned to evaluate whether other effects of endometriotic TIMP1 on ovarian function found in a rat model for human endometriosis [5, 6] will also be MMP dependent or independent. Such studies will also address the autocrine impact of endometriotic lesion TIMP1 on the lesions themselves, as well as paracrine effects on other organs in the peritoneal cavity. In order to modulate TIMP1 as a novel therapeutic approach to ovulatory dysfunction, these issues will need to be resolved.

Together, these data demonstrate the potential of endometriotic TIMP1 in MMP-dependent and multiple MMP-independent roles in misregulating ECM breakdown and breakdown of the follicular wall that goes beyond MMP inhibitory events detrimental to ovulation (Fig. 6). It is possible that multiple mechanisms, both dependent and independent, are exploited to exaggerate these conditions. These mechanisms may be targets for novel therapies to restore ovulatory function in women with endometriosis.

## ACKNOWLEDGMENT

## REFERENCES

1. Sharpe-Timms KL. Using rats as a research model for the study of endometriosis. Ann N Y Acad Sci 2002; 955:318–327; discussion 340–312, 396–406.
2. Vernon MW, Wilson EA. Studies on the surgical induction of endometriosis in the rat. Fertil Steril 1985; 44:684–694.
3. Moon CE, Bertero MC, Curry TE, London SN, Muse KN, Sharpe KL, Vernon MW. The presence of luteinized unruptured follicle syndrome and altered folliculogenesis in rats with surgically induced endometriosis. Am J Obstet Gynecol 1993; 169:676–682.
4. Berkley KJ, Dmitrieva N, Curtis KS, Papka RE. Innervation of ectopic endometrium in a rat model of endometriosis. Proc Natl Acad Sci U S A 2004; 101:11094–11098.
5. Stilley JA, Woods-Marshall R, Sutovsky M, Sutovsky P, Sharpe-Timms KL. Reduced fecundity in female rats with surgically induced endometriosis and in their daughters: a potential role for tissue inhibitors of metalloproteinase 1. Biol Reprod 2009; 80:649–656.
6. Stilley JAW, Birt JA, Nagel SC, Sutovsky M, Sutovsky P, Sharpe-Timms KL. Neutralizing TIMP1 restores fecundity in a rat model of endometriosis and treating control rats with TIMP1 causes anomalies in ovarian function and embryo development. Biol Reprod 2010; 83:185–194.
7. Zhou HE, Nothnick WB. The relevancy of the matrix metalloproteinase system to the pathophysiology of endometriosis. Front Biosci 2005; 10:569–575.
8. Osteen KG, Yeaman GR, Bruner-Tran KL. Matrix metalloproteinases and endometriosis. Semin Reprod Med 2003; 21:155–164.
9. Sharpe-Timms KL, Penney LL, Zimmer RL, Wright JA, Zhang Y, Surewicz K. Partial purification and amino acid sequence analysis of endometriosis protein-II (ENDO-II) reveals homology with tissue inhibitor of metalloproteinases-1 (TIMP-1). J Clin Endocrinol Metab 1995; 80:3784–3787.
10. Sharpe KL, Zimmer RL, Griffin WT, Penney LL. Polypeptides synthesized and released by human endometriosis differ from those of the uterine endometrium in cell and tissue explant culture. Fertil Steril 1993; 60:839–851.
11. Hulboy DL, Rudolph LA, Matrisian LM. Matrix metalloproteinases as mediators of reproductive function. Mol Hum Reprod 1997; 3:27–45.
12. Curry TE Jr, Osteen KG. The matrix metalloproteinase system: changes, regulation, and impact throughout the ovarian and uterine reproductive cycle. Endocr Rev 2003; 24:428–465.
13. Curry TE Jr, Osteen KG. Cyclic changes in the matrix metalloproteinase system in the ovary and uterus. Biol Reprod 2001; 64:1285–1296.
14. Nothnick WB, Soloway P, Curry TE Jr. Assessment of the role of tissue inhibitor of metalloproteinase-1 (TIMP-1) during the periovulatory period in female mice lacking a functional TIMP-1 gene. Biol Reprod 1997; 56:1181–1188.
15. Nothnick WB. Disruption of the tissue inhibitor of metalloproteinase-1 gene results in altered reproductive cyclicity and uterine morphology in reproductive-age female mice. Biol Reprod 2000; 63:905–912.
16. Chirco R, Liu XW, Jung KK, Kim HR. Novel functions of TIMPs in cell signaling. Cancer Metastasis Rev 2006; 25:99–113.
17. Lambert E, Dassé E, Haye B, Petitfrère E. TIMPs as multifacial proteins. Crit Rev Oncol Hematol 2004; 49:187–198.
18. Stetler-Stevenson WG. Tissue inhibitors of metalloproteinases in cell signaling: metalloproteinase-independent biological activities. Sci Signal 2008; 1:re6.
19. Institute of Laboratory Animal Resources (U.S.). Guide for the Care and Use of Laboratory Animals. Washington, D.C.: National Academy Press; 1996.
20. Seo DW, Li H, Guedez L, Wingfield PT, Diaz T, Salloum R, Wei BY, Stetler-Stevenson WG. TIMP-2 mediated inhibition of angiogenesis: an MMP-independent mechanism. Cell 2003; 114:171–180.
21. Wingfield PT, Sax JK, Stahl SJ, Kaufman J, Palmer I, Chung V, Corcoran ML, Kleiner DE, Stetler-Stevenson WG. Biophysical and functional characterization of full-length, recombinant human tissue inhibitor of metalloproteinases-2 (TIMP-2) produced in *Escherichia coli*. J Biol Chem 1999; 274:21362–21368.
22. Sharpe KL, Bertero MC, Lyon BP, Muse KN, Vernon MW. Follicular atresia and infertility in rats treated with a gonadotropin-releasing hormone antagonist. Endocrinology 1990; 127:25–31.
23. Pelch KE, Schroder AL, Kimball PA, Sharpe-Timms KL, Davis JW, Nagel SC. Aberrant gene expression profile in a mouse model of endometriosis mirrors that observed in women. Fertil Steril 2010; 93:1615–1627.e18.
24. Huang da W, Sherman BT, Lempicki RA. Systematic and integrative analysis of large gene lists using DAVID bioinformatics resources. Nat Protoc 2009; 4:44–57.
25. Huang da W, Sherman BT, Lempicki RA. Bioinformatics enrichment tools: paths toward the comprehensive functional analysis of large gene lists. Nucleic Acids Res 2009; 37:1–13.
26. Rasband WS. Image J. U.S. National Institutes of Health, Bethesda, Maryland, USA, http://imagej.nih.gov/ij/, 1997–2011.
27. Knight PG, Glister C. TGF-β superfamily members and ovarian follicle development. Reproduction 2006; 132:191–206.
28. Donnez J, Thomas K. Incidence of the luteinized unruptured follicle syndrome in fertile women and in women with endometriosis. Eur J Obstet Gynecol Reprod Biol 1982; 14:187–190.
29. Kaya H, Oral B. Effect of ovarian involvement on the frequency of luteinized unruptured follicle in endometriosis. Gynecol Obstet Invest 1999; 48:123–126.
30. Mio Y, Toda T, Harada T, Terakawa N. Luteinized unruptured follicle in the early stages of endometriosis as a cause of unexplained infertility. Am J Obstet Gynecol 1992; 167:271–273.
31. Plendl J. Angiogenesis and vascular regression in the ovary. Anat Histol Embryol 2000; 29:257–266.
32. Neufeld G, Cohen T, Gengrinovitch S, Poltorak Z. Vascular endothelial growth factor (VEGF) and its receptors. FASEB J 1999; 13:9–22.
33. Ravindranath N, Little-Ihrig L, Phillips HS, Ferrara N, Zeleznik AJ. Vascular endothelial growth factor messenger ribonucleic acid expression in the primate ovary. Endocrinology 1992; 131:254–260.
34. Friedman CI, Seifer DB, Kennard EA, Arbogast L, Alak B, Danforth DR.

Elevated level of follicular fluid vascular endothelial growth factor is a marker of diminished pregnancy potential. Fertil Steril 1998; 70:836–839.

35. McLaren J. Vascular endothelial growth factor and endometriotic angiogenesis. Hum Reprod Update 2000; 6:45–55.

36. Fujii EY, Nakayama M, Nakagawa A. Concentrations of receptor for advanced glycation end products, VEGF and CML in plasma, follicular fluid, and peritoneal fluid in women with and without endometriosis. Reprod Sci 2008; 15:1066–1074.

37. Pankov R, Yamada KM. Fibronectin at a glance. J Cell Sci 2002; 115:3861–3863.

38. Curry TE, Song L, Wheeler SE. Cellular localization of gelatinases and tissue inhibitors of metalloproteinases during follicular growth, ovulation, and early luteal formation in the rat. Biol Reprod 2001; 65:855–865.

39. Ricciardelli C, Rodgers RJ. Extracellular matrix of ovarian tumors. Semin Reprod Med 2006; 24:270–282.

40. Dassé E, Bridoux L, Baranek T, Lambert E, Salesse S, Sowa ML, Martiny L, Trentesaux C, Petitfrère E. Tissue inhibitor of metalloproteinase-1 promotes hematopoietic differentiation via caspase-3 upstream the MEKK1/MEK6/p38alpha pathway. Leukemia 2007; 21:595–603.

41. Li G, Fridman R, Kim HR. Tissue inhibitor of metalloproteinase-1 inhibits apoptosis of human breast epithelial cells. Cancer Res 1999; 59:6267–6275.

42. Li F, Curry TE Jr. Regulation and function of tissue inhibitor of metalloproteinase (TIMP) 1 and TIMP3 in periovulatory rat granulosa cells. Endocrinology 2009; 150:3903–3912.

43. Smith MF, McIntush EW, Ricke WA, Kojima FN, Smith GW. Regulation of ovarian extracellular matrix remodelling by metalloproteinases and their tissue inhibitors: effects on follicular development, ovulation and luteal function. J Reprod Fertil Suppl 1999; 54:367–381.

44. Jung KK, Liu XW, Chirco R, Fridman R, Kim HR. Identification of CD63 as a tissue inhibitor of metalloproteinase-1 interacting cell surface protein. EMBO J 2006; 25:3934–3942.

45. Ackerman RC, Murdoch WJ. Prostaglandin-induced apoptosis of ovarian surface epithelial cells. Prostaglandins 1993; 45:475–485.